Periodica Polytechnica
Civil Engineering

61 (4). pp. 762–769, 2017
https://doi.org/10.3311/PPci.10349

Resonant Column Test on the Frozen Silt Soil Modulus and Damping at Different Temperatures

Xiaobo Yu[1], Rui Sun[1*], Xiaoming Yuan[1], Zhuoshi Chen[1], Jiuqi Zhang[1]

RESEARCH ARTICLE

Received 03 December 2016; Revised 06 January 2017; Accepted 21 February 2017

Abstract

The shear modulus and damping ratio of frozen soil are the basic parameters of its dynamic properties and are often tested with the dynamic triaxial apparatus. However, the resonant column apparatus is more suitable for the testing at the micro-strain level. A resonant column apparatus was here used to identify the varying modes with negative temperature of the initial shear modulus, modulus ratio, and damping ratio of frozen silt. Correction factor curves indicate that the temperature has a great effect on the shear modulus and damping ratio of frozen silt. The curves also show that, within the sensitive stage, the temperature significantly affects the modulus and damping. Within the insensitive stage, the modulus and damping were insensitive to the temperature. The experimental results and analysis given here provide support for improving seismic design codes and offer reasonable parameters for seismic response analysis in engineering construction in cold regions.

Keywords

resonant column, frozen silt, shear modulus, damping ratio, Hardin-Drnevich model

[1]Key Laboratory of Earthquake Engineering and Engineering Vibration, Institute of Engineering Mechanics, China Earthquake Administration, Harbin 150080, China.

[*]Corresponding author, email: iemsr@163.com

1 Introduction

Large frozen regions are distributed around the world, as in subarctic countries [1,2]. Compared to soil under normal conditions (15°C to 25°C), under which pore water remained in a liquid state inside the soil, the dynamics of frozen ground varies significantly with the seasons, resulting in different vibratory responses for building and civil engineering structures; even seismic damage is related to the season. The seasonal influences were demonstrated in the seismic damage caused by the earthquake swarm that occurred in Dedu county, China, in 1986. These earthquakes occurred in the summer and winter; the stiffer buildings suffered more during the winter earthquake events, while the more flexible buildings were damaged during the summer events [3]. Research on the frequency of building during an Alaskan winter illustrates that the first-order mode frequency of reinforced concrete frame structures with a shallow foundation increases nearly 50% over construction performed during the summer [4].

There are many researchers studying the shear modulus and damping ratio of normal soil [5–10], also some researchers have made significant achievements using specific soils [11–15]. Common used testing devices are resonant column apparatus (RCA) and dynamic triaxial apparatus (DTA), and the utilization frequency of DTA is higher than RCA. But in fact, the resonant column test (RCT) at normal temperatures (15°C to 25°C) is relatively reliable, and certain codes, such as the Chinese standard (SL237-1999) and the American standard (D4015-92) [16,17], have proven to be useful.

In contrast, research on the shear modulus and damping ratio of frozen soil is limited [3,18–20]. These researches revealed each factor that affects the modulus and damping to a different extent. However, the equipment performance and technological level required for a low temperature environment are more complex than those found in normal temperature tests. For all of the research noted above, there is a limit to the equipment's capabilities as well as some issues with the methodology, as shown in the following list.

(1) Most of the modulus and damping ratio values of the frozen soil were obtained with the DTA. In these tests, the shear modulus was transformed from the elastic modulus by assuming Poisson's ratio, whose reliability needs to be reconsidered. The test scope of the strain amplitude for the dynamic triaxial apparatus is from 10^{-4} to 10^{-2}, while the strain amplitude inside the frozen specimen during a seismic event is relatively small, which results in the interpolation of the shear modulus and damping ratio curves for a low-strain scope.

(2) The confining pressure employed in most low-temperature triaxial tests is higher than that found in a natural situation, usually 0.3 MPa to 3.5 MPa. In general, the maximum depth of the seasonally frozen soil is about 10 meters [22], so the corresponding confining pressure is about 100 kPa. The excessive confining pressure used in the prior laboratory tests is not suitable for evaluating frozen soil.

(3) Some parts of the sample preparation process for the low-temperature dynamic triaxial test were conducted in a refrigerator; afterwards, the researchers installed the samples in a pressure chamber. This activity requires superior experimental skills, as a laboratory technician needs to take the frozen specimen and assemble components of the apparatus in a short time without the specimen melting. In a natural setting, the freezing process of soil proceeds under pressure from the surrounding soil, which is inconsistent with the sample preparation process found in these laboratories.

(4) Compared to the DTA, the RCA is mechanically reliable and convenient for use in analysis. The RCA is ideal for capturing the dynamic modulus and damping ratio at a strain amplitude scope from 10^{-6} to 5×10^{-4}; its test results can be utilized directly in the seismic response analysis of layered soil. The shear strain inside a frozen soil layer during a vibration event, like earthquake, is much smaller than that under unfrozen conditions, so the RCA is superior in obtaining the dynamic modulus and damping ratio of this stiff soil type. However, the excitation force of the magnet coil and coarse filtering noise ability of the data acquisition equipment used in the prior research were limited. The small soil sample amounts taken with the RCA that were used to reveal the dynamic modulus and damping ratio of the frozen soil sample were inadequate, as were the narrow scope of the shear strain amplitude and lack of precise temperature control [18]. Test results of Al-Hunaidi et al [18] and Zhang [21] are presented in the later chapter, which verify results in the present study and reveal the advantages of RCA in micro-strain experiments.

(5) There was an absence of an acknowledged low-temperature experimental technique, regardless of the type of apparatus utilized. The lack of an appropriate technique may have resulted in large discrepancies in the data. Also, the absence of uniform technique standards results in too many testing errors, and such experimental results lack comparability.

A set of test techniques was explored in this research. These techniques were based on a low-temperature RCA. We explore the effects of the experimental parameters on the testing repeatability, such as the confining medium and freezing duration. The basic mode of the negative temperature effect on the shear modulus and damping ratio was elucidated, and the corresponding empirical correction factor concepts were proposed. This work lays the foundation for the modification of the seismic design spectrum in seasonal frozen areas, and provides support for correctly estimating the effects of seismic waves in building design.

2 RCA for the low temperature test

Global Digital Systems Instruments, Ltd. (Hampshire, United Kingdom) has specially developed a low-temperature RCA for the work in 2012 (Fig. 1). This equipment can precisely control and measure a number of parameters, including the confining pressure, back pressure, back volume, pore pressure, and exciter coil voltage through the software programs GDSLAB and GDSRCA. The control module for the temperature provides a reliable low-temperature environment that surrounds the specimen. The main performance parameters of the RCA can be seen in Table 1.

A Thermo Scientific HAAKE Bath was employed as the temperature control system, with a minimum temperature of −40 ± 0.01°C. One end of the cooling pipes was connected to the Bath and the other end held the soil specimen in the cell; these pipes were used to freeze the specimen, where the copper pipes were wound manually. A heat preservation cover enclosed the cell, ensuring that most of the cold energy was kept inside the cell. A thermocouple was placed inside the cell and was used to measure the cell environment's temperature. The temperature value was read and recorded in real time with GDSLAB. The axial displacement was measured by a linear variable differential transformer on the top of the specimen, which reflected the consolidation and freezing process.

Table 1 Low-temperature RCA main performance parameters

Property	Information
Specimen size	Φ50 × 100 mm
Confining pressure	0 – 1000 ± 1 KPa
Excitation voltage	0.001 – 1 V
Excitation frequency	5 – 1000 Hz
Frequency step	> 0.01 Hz
Shear strain range	10^{-7} – 10^{-4}
Temperature in the chamber	> −25 ± 1 °C

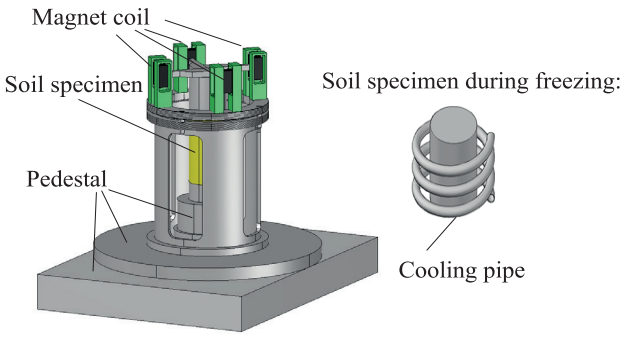

Fig. 1 Low-temperature RCA schematic diagram

3 Specimen preparation

Silt was taken from a depth of 3 meters underground in the Hulan District of Harbin, China. The grading curve and physical properties of the specimen are shown in Fig. 2 and Table 2, respectively. All the specimens were remoulded by compacting them into five layers according to the Chinese standard (GB/T50123-1999) [23]. Afterwards, the specimens were air exhausted by vacuum pump for at least 12 hours to eliminate air in the pores. Water was added to the vacuum chamber until the specimens were submerged; this saturation lasted for a minimum of 48 hours in order to ensure sufficient water absorption. The mold was removed and the specimens were installed at the pedestal of the RCA before the test. The consolidation procedure was conducted at 100 kPa for at least 8 hours, as the back volume and axial displacement tended to stabilize.

Table 2 Physical properties of the silt

Density g/cm³	Specific gravity	Moisture content %	Saturation %	Plastic limit %	Liquid limit %	Plasticity Index
2.07	2.70	26.5	88	21.2	30.5	9.3

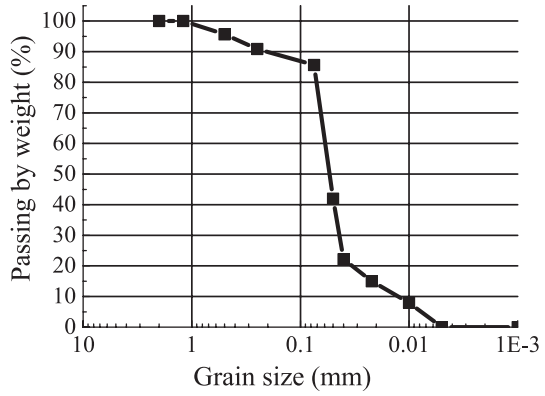

Fig. 2 Grading curve of the silt

4 Confining medium selection

Membranes manufactured from natural rubber (NR) age quickly when exposed to the negative temperatures found in cold environments, resulting in the reduction of their elasticity and hermeticity. These may lead to inconsistent degrees of consolidation and freezing. The inconsistent experimental condition rendered the results of the test unreliable. The basic requirement for the confining liquid in a low-temperature environment is its low freezing point, since otherwise ice crystals in the liquid would seriously impact the test results. Some schemes have been proposed for a comparative test (please see Table 3).

An alternative confining liquid is needed for low-temperature experiments, as water (which is commonly used) is inadequate. Compacted air, anti-freeze, and silicon oil were chosen as the confining medium for the comparative test. Anti-freeze is often used in automobile engine cooling systems and has a −35°C freezing point. Silicon oil is often used as a lubricant or hydraulic fluid since it is nontoxic and has a low freezing point. It should be noted that confining pressure in the test was only 100 kPa, so it did not stress the transmission performance of the silicon oil. The coordinating silicon oil scheme, CR (Chloroprene Rubber) membrane, was employed since it is more easily adapted to the oil and low-temperature environment than the NR membrane.

There were three parallel tests for each scheme that evaluated the effects of each medium. Figure 3 shows the results of schemes 1–3. In Fig. 3a and 3c, a great difference appears among the parallel results. Figure 3b and 3d show that the damping ratio curves are dispersed. Figure 3e and 3f show that all of the data are close enough to the requirements needed for the test.

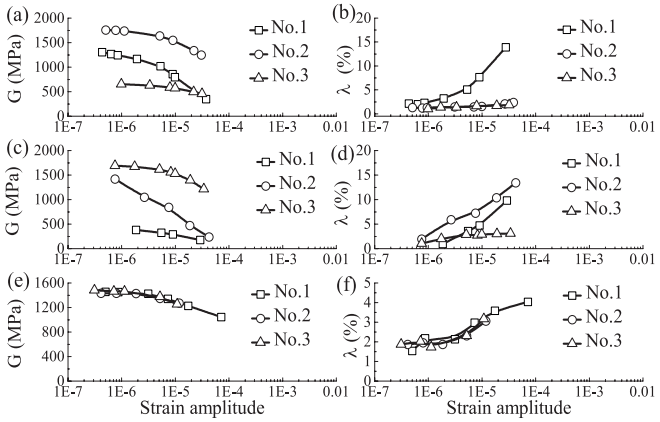

Fig. 3 Test results of scheme 1~3. (a), (b) for scheme 1. (c), (d) for scheme 2. (e), (f) for scheme 3.

Figures 3a~3d indicate that different degrees of freezing cause the dispersion of the initial modulus (G_{max}) data. The errors originated from the different degrees of consolidation and freezing for the damping ratio (λ) data. Anti-freeze and compacted air leakage can directly influence the freezing point and consolidation degree of the soil, which is likely to occur in schemes 1 and 2. The test results for scheme 3 are more reliable than those of the other schemes. The silicon oil or the CR membrane or their combined effects maintain the hermeticity in the negative temperature environment in scheme 3.

Based on the comparative test results shown above, all of the following tests employed scheme 3.

Table 3 Selection scheme of the confining pressure medium

Scheme	Pressure transmitting medium	Rubber membrane
1	Antifreeze	Natural rubber
2	Compressed air	Natural rubber
3	Silicon oil	Chloroprene rubber

5 Freezing duration selection

The freezing duration has a great influence on the frozen soil's dynamic properties, as the state of the ice content and ice crystal growth are dependent on the time it takes the soil to freeze completely. The mechanical properties of a soil specimen change gradually during the freezing process. The axial displacement works as a measurable indicator for the degree of freezing, as shown in Fig. 4. The temperature and displacement time-history curves started with the end of the consolidation. Meanwhile, the cooling bath system was activated. The positive values of displacement in Fig. 4 refer to the sedimentation and negative values are the frost heaving.

Figure 4 presents two stages of freezing: development and stabilization. A plateau region can be seen starting at 1–2 hours and represents a continuous adjustment and balancing procedure between the cooling bath and confining medium.

Figure 4 shows that the axial displacement relates to the temperature. The axial displacement line stays flat starting at 8 hours and the temperature falls to nearly −4°C at the same time. Later, from the 8th hour to the 12th hour, frozen heaving occurs as the axial displacement falls rapidly. The temperature at this stage changes slowly. After the 12th hour, the frozen heaving ends with a stable axial displacement and temperature. Figure 4 shows that at the 24th hour, the displacement of the specimen and temperature of the confining medium are flat. The freezing procedure was completed in 24 hours.

Longer freeze durations result in a greater stabilization of the ice content. It takes time to balance the water migration inside the specimen. However, it is impossible to ensure freezing over a long period of time, as a long testing time is inefficient. Other researchers [20, 21, 24] have used freeze durations of 24~48 hours. The comparative tests between the freeze durations of 24 hours and 48 hours were conducted to confirm the applicability of the 24-hour duration. Figure 5 presents a set of results at −3°C, in which data are close to each other. This one aspect demonstrates the rationality of the 24-hour duration.

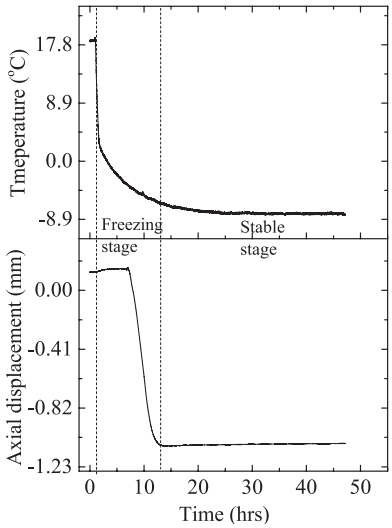

Fig. 4 The relationship between the freeze duration and axial displacement after consolidation

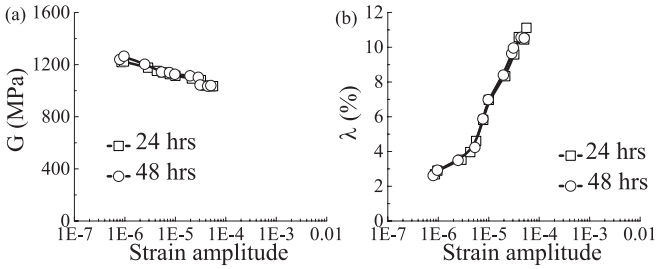

Fig. 5 The freezing duration affects the test results (−3 °C): a) Shear modulus, (b) Damping ratio

6 Temperature effects on the modulus and damping

6.1 Sensitive stage

A low temperature RCA was used to examine the effect of the temperature in the present study.

In the Chinese standard (GB/T50123-1999), the initial temperature of freezing is determined by the jump in the electromotive force. However, for the RCT at relative higher negative temperatures, the results are still the same as those at unfrozen temperatures. This is because the freezing degree of the specimens at this temperature is low. The temperature around this initial freezing point is called the sensitive range. A series of temperatures was set up to present this phenomenon (Fig. 6).

Figure 6 shows that the results at −1.4°C are similar to those at unfrozen temperatures (20°C), where both values for Gmax are less than 100 MPa, much lower than those at other negative temperatures. The results for the −1.4°C shear modulus ratio and damping ratio are similar to those at normal temperatures. The test results change significantly in the ranges from −1.4°C to −2.2°C and −2.2°C to −3.0°C. The results changed slowly as the temperature decreased to under −3.0°C. These results suggest that the temperature range, from normal temperatures to about −4.0°C, is the sensitive range of this silt, where only small parts of the specimen are frozen and the mechanical properties of the ice crystals in the specimen are unstable.

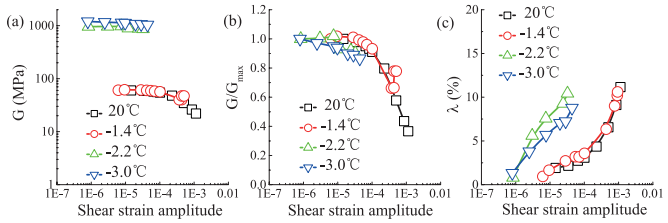

Fig. 6 Change of the shear modulus and damping ratio in the frozen phase: (a) Shear modulus, (b) Shear modulus ratio, and (c) Damping ratio

6.2 Insensitive stage

The dynamic performance of the frozen specimen became stable when the temperature decreased below the sensitive range. The stable range occurred outside the sensitive range. Four negative temperatures, −15°C, −10°C, −5°C, and −3°C, were set for the RCT and normal temperatures were set for the control group. Parallel tests were set for each temperature, with a 100 kPa confining pressure (some are shown in Figs. 7).

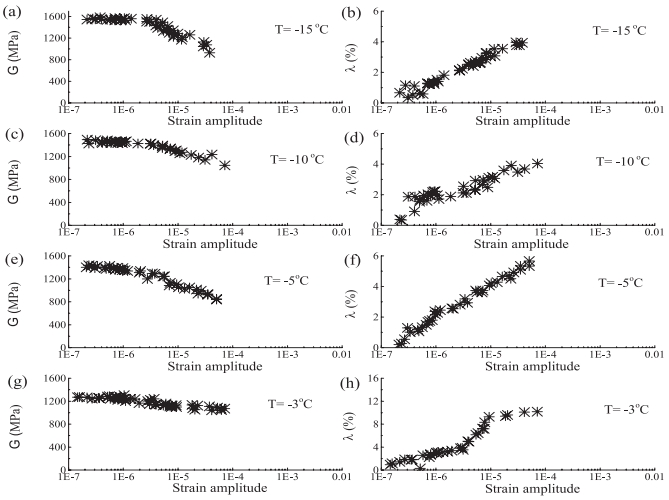

Fig. 7 Test results at different temperature

Figures 7 illustrate that the test results are reliable, since the results of the 3 parallel tests were close to each other. It should be noted that the discretization error exists and is larger than that found in the normal temperature test. Supposedly, the discretization error of the sample preparation is enlarged when the sample is frozen; the error exists when the components of the RCA are installed. The aging and deformation of the CR membrane at negative temperatures and in the oily environment also affect the test results.

The fitting curve shown in the figures is the Hardin-Drnevich hyperbolic model [25], which describes the modulus ratio and damping ratio. The Hardin-Drnevich model parameters of the three parallel test results were averaged and the dynamic nonlinear curves at certain temperatures were acquired. The measured strain amplitude was distributed at an interval of 10^{-7}~10^{-4}. The values of the strain amplitude beyond 10^{-4} were obtained through the interpolation of the fitting curves. The interpolation was reliable, as some research [19,20] with DTA on frozen soil were conducted under strain amplitudes larger than 10^{-4} and those results match the Hardin-Drnevich model.

The Hardin-Drnevich model is shown in Eqs. (1) and (2):

In Eqs.(1) and (2), G_{max} is the initial shear modulus (MPa), γ is the shear strain amplitude, γ_r is the reference shear strain, λ_{max} is the maximum damping ratio (the damping ratio at γ = 0.01, in practice), and n is a fitting parameter. The parameters in Eqs. (1) and (2) are presented in Table 4.

$$\frac{G}{G_{max}} = \frac{1}{1+\gamma/\gamma_r} \tag{1}$$

$$\lambda = \lambda_{max}(1-\frac{G}{G_{max}})^n \tag{2}$$

Table 4 Parameters of the frozen silt modulus ratio and damping ratio curves at different temperatures

Temperature °C	G_{max} MPa	γ_r	λ_{max}	n
−15	1539.2	6.312×10^{-5}	0.073	0.42
−10	1467.4	6.670×10^{-5}	0.078	0.36
−5	1341.8	7.520×10^{-5}	0.106	0.44
−3	1238.4	9.354×10^{-5}	0.116	0.36
Room temperature (15°C to 25°C)	64.2	6.602×10^{-4}	0.183	0.60

Figure 8 presents the fitting curves with the detailed information from Table 4. It is evident that the curves of the frozen specimen are quite different from those found at normal temperatures (15°C to 25°C). The modulus ratio (G/G_{max}) values of the normal temperature are much higher than those of the negative temperature values. The damping ratio (λ) values of negative temperatures are higher than those of normal temperatures in the strain interval of 10^{-6} to 5×10^{-4}, which are unusual and will be discussed later. For λ at γ = 0.01, the values for the normal temperatures are larger than the values for the negative temperatures, and they decrease with the decreasing temperature.

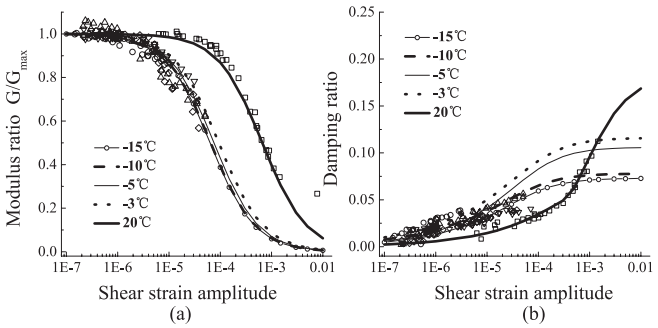

Fig. 8 Nonlinear curves at different temperatures: (a) Modulus ratio curves and (b) Damping ratio curves

Compared to soil under normal temperature conditions, the G/G_{max} of the frozen soil decreases more rapidly with the increasing strain amplitude. Although the rate of decrease is quite high, the G of the frozen specimen is larger than that found under normal temperature conditions because the G_{max} of frozen soil is significantly magnified. It is difficult for the RCT for frozen soil to reach a strain amplitude exceeding 10^{-4}, so frozen soil can still be regarded as a stiff material.

The damping ratio curve changes significantly for specimens in unfrozen conditions relative to those in freezing conditions. The curve for normal temperatures is lower than that for negative temperatures during a certain range of the strain amplitude; however, with the increasing amplitude, the normal curve becomes gradually higher than the curve for the negative temperatures. This may be due to the damping mechanism inside the specimen at unfrozen temperatures, where the particle deformation and the pore water's viscous force constitute the energy dissipation. At the micro-strain amplitude, the main energy dissipation is caused by the viscous force of the pore water and bound water. This dissipation mode is not useful for making comparisons with the particle deformation mode. When the strain amplitude is larger, the deformation mode can be substituted for the viscous mode, becoming generalized inside the specimen with the result of rapidly increasing the damping ratio. The energy dissipation mode is only the particle deformation that remained in the frozen specimen, which shows more energy dissipation than that found with an unfrozen specimen at the same micro-strain amplitude.

7 Discussion

Al-Hunaidi et al. [18] took undisturbed frozen samples from two adjacent boreholes in the winter. The samples consisted of clay with some sand and were cut into the appropriate size for the low temperature RCT. The test was performed with a 14 kPa confining pressure and −9°C environmental temperature. The samples were placed at 22°C for four days before being tested. Their work provided 3 strain amplitude test results at low and normal temperatures. The data are fitted using Eqs. (1) and (2), as shown in Fig. 9.

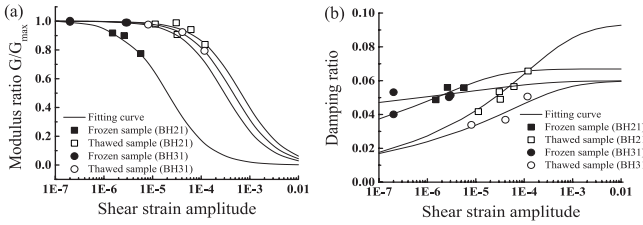

Fig. 9 Comparison of the frozen and ordinary soil non-linear curves by resonant column test (data from Al Hunaidi et al. [18]): (a) G/G_{max} and (b) Damping ratio

Figures 9a and 9b show the large difference in the decreasing rates between the two frozen sample results, which may be the result of the uncertainty of the natural samples' interior micro-structure and defects in the experiment operations. The stiffness of the frozen sample was larger than that of the sample taken at an unfrozen temperature, so the stability and accuracy of these freezing tests were difficult to guarantee. Their results show that the shear modulus and damping ratio curves of the frozen and thawed samples are quite different, and the thawed G/G_{max} curves are higher than those of the frozen samples. The frozen damping ratio curves are higher than the thawed curves at a strain amplitude under about 10−4. These results agree with the results of the present study.

Zhang [21] conducted dynamic triaxial tests on frozen sand with a 2-Hz loading frequency and 0.3-MPa confining pressure. Zhang [21] developed equations for the shear modulus and damping ratio evaluation, which were used for the curves in Fig. 10; in this figure, the initial shear modulus G_{max} increases and the maximum damping ratio decreases with the decreasing temperature. These outcomes qualitatively correspond to the results from our experiments in section 6.2. However, the decreasing rate of the G/G_{max} curves (shown in Fig. 10b) are rather different than ours, where the value stays stable at $\gamma < 10{-}3$. There is a rapid decreasing stage in the micro-strain amplitude range found in both Al-Hunaidi et al.'s RCT results (Fig. 9) and our results in section 6.2 (Fig. 8). Zhang's results can be explained as the scarce strain amplitude with the dynamic triaxial test results and unreliable curve fitting at the micro-strain amplitude level. The 0.3 MPa confining pressure in Zhang's work is different from the 100 kPa confining pressure used in our work.

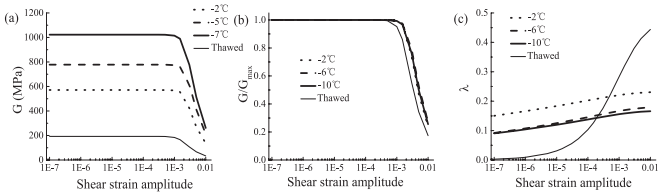

Fig. 10 Shear modulus, modulus ratio, and damping ratio curves influenced by temperature (data from Zhang [21]): (a) Shear modulus, (b) Modulus ratio, and (c) Damping ratio

Using the dynamic shear modulus and damping ratio at different temperatures from the results in section 6.2, we derived the temperature correction coefficients that work in the Hardin-Drnevich model.

$$G'_{max} = \alpha_G \times G_{max} \tag{3a}$$

$$\gamma'_r = \alpha_\gamma \times \gamma_r \tag{3b}$$

$$\lambda'_{max} = \alpha_\lambda \times \lambda_{max} \tag{3c}$$

In Eq. (3), α_G, α_γ, and α_λ are the correction coefficients of the initial shear modulus, reference shear strain, and maximum damping ratio, respectively. G_{max}', γ_r', and λ_{max}' are the initial shear modulus, reference shear strain, and maximum damping ratio at negative temperatures, respectively. G_{max}, γ_r, and λ_{max} are the initial shear modulus, reference shear strain, and maximum damping ratio at normal temperatures (15°C to 25°C).

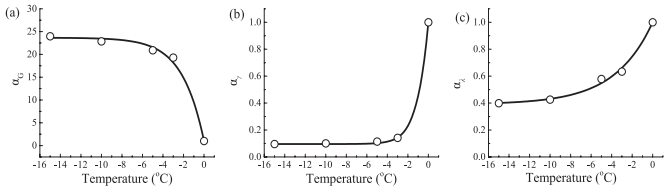

Fig. 11 Shear modulus and damping ratio correction coefficient curves at subzero temperatures: (a) G_{max} correction curve, (b) α_γ correction curve, and (c) α_λ correction curve

The Boltzmann and index formulas were employed using the data we obtained, and the α_G, α_γ, and α_λ curves are shown in Fig. 11.

Figure 11a shows that α_G is significantly magnified (24 times), which reflects the effects of the ice formation. α_G remained in the rapid increase stage between −4°C to 0°C, which suggests that the ice-water phase change inside the specimen is the main part of the modulus amplification. This phenomenon can be interpreted as the unfrozen pore water content decrease with the increasing pore ice cementation. When the freezing process is close to finishing, the pore ice content stabilized and the frozen specimen is no longer sensitive to lower temperatures.

When the shear modulus decreases to half of the initial value and the strain amplitude increases, the strain amplitude at the time is defined as the reference strain γ_r. The γ_r reflects the fragility of the specimen and the decay rate of the shear modulus. Figure 11b shows that the α_γ curve is less than 1.0, where the fragility of the frozen specimen is enhanced. The α_γ curve varies from 1.0 to about 0.1, a significant reduction of 90%. A rapid decreasing stage between −4°C to 0°C occurs where the ice-water phase change was generated and the α_γ remained the same with the decreasing temperature. In the frozen state, the soil skeleton is enhanced by the pore ice, which also limits the deformation ability of the skeleton. For the same strain amplitude, the normal soil skeleton maintains its stability by soil particle deformation, or particle displacement. Frozen soil contains a large amount of pore ice and the deformation and displacement ability of the particles are limited by the transformation from viscoelasticity to fragility.

The maximum damping ratio λ_{max} is the ratio between the damping coefficient and corresponding critical damping coefficient. Briefly, the maximum damping ratio is the damping ratio when G/G_{max} tends to zero (Eq. (2)). In Fig. 11c, the α_γ curve is less than 1.0 and part of a greatly decreasing stage, with a 60% reduction in amplitude. The damping ratio is a description of the energy dissipation. The differences between the damping mechanisms in the frozen and unfrozen specimens are due to the effects of the ice. The ice enhanced the structure of the soil skeleton, the particle movements were restricted, and the pore fluid motion tended to disappear, so the energy dissipation was reduced and the maximum damping ratio decreased at the macro level.

8 Conclusions

The technique for the low temperature RCT is more complex than the technique used for an unfrozen RCT. In the experiments, CR membrane and silicon oil were used as the medium transferring the confining pressure. The duration of the freezing time was 24 hours. These measures achieved favorable results.

A negative temperature has a great effect on the G_{max}, G/G_{max}, and λ. The G_{max} increases with the decreasing temperature while the γ_r decreases. The negative temperature λ curve is higher than the normal temperature ratio curve in the strain range of 10^{-6} to 5×10^{-4}, while the normal temperature curve gradually surpasses the frozen one in the strain range larger than 5×10^{-4}.

The sensitive stage of the initial modulus correction coefficient α_G was 0°C ~ −4.0°C for the frozen silt specimen used in this work. The stable stage was lower than −4.0°C, and the initial modulus gently increased with the decreasing temperature.

The sensitive and stable stage for the reference strain correction coefficient α_γ was 0°C ~ −4.0°C and < −4.0°C, the same as that for the initial modulus.

The exponential equation is suitable for the description of the maximum damping ratio correction coefficient α_λ. The α_λ curve becomes flatter with the varying temperature, unlike the α_G and α_γ curves. However the damping ratio curve needs further study, as there is some divergence on the damping mechanism.

Acknowledgement

This research was supported by the Scientific Research Fund of the Institute of Engineering Mechanics, China Earthquake Administration (Grant No. 2016A02) and the National Natural Science Foundation of China (Grant No. 51378164). The authors also thank LetPub (www.letpub.com) for its linguistic assistance during the preparation of this manuscript.

References

[1] Harris, C., Arenson, L.U., Christiansen, H.H., Etzelmüller, B., Frauenfelder, R., Gruber, S., Haeberli, W., Hauck, C., Hölzle, M., Humlum, O., Isaksen, K., Kääb, A., Kern-Lütschg, M.A., Lehning, M., Matsuoka, N., Murton, J.B., Nötzli, J., Phillips, M., Ross, N., Seppälä, M., Springman, S.M., Vonder Mühll, D. "Permafrost and climate in Europe: Monitoring and modelling thermal, geomorphological and geotechnical responses ". *Earth-Science Reviews*, *92*(3), pp. 117–171. 2009. https://doi.org/10.1016/j.earscirev.2008.12.002

[2] Batir, J. F., Hornbach, M. J., Blackwell, D. D. "Ten years of measurements and modeling of soil temperature changes and their effects on permafrost in Northwestern Alaska". *Global & Planetary Change*, *148*, pp. 55–71. 2016. https://doi.org/10.1016/j.gloplacha.2016.11.009

[3] Xu, X., Zhong, C., Chen, Y. , Zhang, J. "Research on dynamic characters of frozen soil and determination of its parameters". *Chinese Journal of Geotechnical Engineering*, *20*(5), pp. 80–84. 1998. (In Chinese with English abstract) http://www.cgejournal.com/EN/Y1998/V20/I5/80

[4] Xiong, F., Yang, Z., Xu, G. "Seasonally Frozen Soil Effects on the DynamicBehavior of Building Structures". In: The 14th World Conference on Earthquake Engineering. Beijing, China, Oct. 12–17. 2008. http://www.iitk.ac.in/nicee/wcee/article/14_S09-005.pdf

[5] Yuan, X., Sun, R., Sun, J., Meng, Sj., Shi, Zj. "Laboratory experimental study on dynamic shear modulus ratio and damping ratio of soils". *Earthquake Engineering and Engineering Vibration*, *20*(4), pp. 133–139. 2000.http://en.cnki.com.cn/Journal_en/C-C038-DGGC-2000-04.htm (In Chinese with English abstract)

[6] Assimaki, D., Kausel, E. "An equivalent linear algorithm with frequency- and pressure-dependent moduli and damping for the seismic analysis of deep sites". *Soil Dynamics & Earthquake Engineering*, *22*(9–12), pp. 959–965. 2002. https://doi.org/10.1016/S0267-7261(02)00120-3

[7] Mayoral, J. M., Castañon, E., Alcantara, L., Tepalcapa, S. "Seismic response characterization of high plasticity clays". *Soil Dynamics & Earthquake Engineering*, *84*, pp. 174–189. 2016. https://doi.org/10.1016/j.soildyn.2016.02.012

[8] Keshavarz, A., Mehramiri, M. "New Gene Expression Programming models for normalized shear modulus and damping ratio of sands". *Engineering Applications of Artificial Intelligence*, *45*, pp. 464–472. 2015. https://doi.org/10.1016/j.engappai.2015.07.022

[9] Kong G Q, Zhou L D, Wang Z T, Yg, G., Li, H. "Shear modulus and damping ratios of transparent soil manufactured by fused quartz.". *Materials Letters*, *182*, pp. 257–259. 2016. https://doi.org/10.1016/j.matlet.2016.07.012

[10] Senetakis K, Anastasiadis A, Pitilakis K. "Normalized shear modulus reduction and damping ratio curves of quartz sand and rhyolitic crushed rock". *Soils & Foundations*, *53*(6), pp. 879–893. 2013. https://doi.org/10.1016/j.sandf.2013.10.007

[11] Wang, Z. J., Luo, Y. S., Guo, H., Tia, H. "Effects of initial deviatoric stress ratios on dynamic shear modulus and damping ratio of undisturbed loess in China". *Engineering Geology*, 143–144, pp. 43–50. 2012. https://doi.org/10.1016/j.enggeo.2012.06.009

[12] Mosallamy, M. E., Fattah, T. T. A. E., Khouly, M. E. "Experimental study on the determination of small strain-shear modulus of loess soil". *HBRC Journal*, *35*(2), pp. 181–190. 2015. https://doi.org/10.1016/j.hbrcj.2014.11.010

[13] Chattaraj R, Sengupta A. "Liquefaction potential and strain dependent dynamic properties of Kasai River sand". *Soil Dynamics & Earthquake Engineering*, 90, pp. 467–475. 2016. https://doi.org/10.1016/j.soildyn.2016.07.023

[14] Elia G, Rouainia M. "Investigating the cyclic behaviour of clays using a kinematic hardening soil model". *Soil Dynamics & Earthquake Engineering*, *88*, pp. 399–411. 2016. https://doi.org/10.1016/j.soildyn.2016.06.014

[15] Yılmaz M T, Zehtab K H. "A practical method for utilization of commercial cyclic testing apparatuses for computation of site response in central Adapazari". *Soil Dynamics & Earthquake Engineering*, *63*(63), pp. 203–216. 2014. https://doi.org/10.1016/j.soildyn.2014.04.003

[16] American Society of Testing Materials. "D 4015-92 Standard test methods for modulus and damping of soils by the resonant-column method". Philadelphia: American Society for Testing and Materials, 2000. http://www.dres.ir/fanni/khak/DocLib4/D%204015%20%E2%80%93%2092%20R00%20%20;RDQWMTU_.pdf

[17] The Ministry of Water Resource of the People's Republic of China. "Specification of soil test (SL237-1999)". Beijing: China Water & Power Press, pp. 277–293. 1999. (In Chinese)

[18] Al-Hunaidi, M. O., Chen, P. A. , Rainer, J. H., Tremblay, M. "Shear moduli and damping in frozen and unfrozen clay by resonant column test". *Canadian Geotechnical Journal*, *33*(3), pp. 510–514. 1996. https://doi.org/10.1139/t96-073

[19] Qi, J., Ma, W., Sun, C., Lanmin, W. "Ground motion analysis in seasonally frozen regions". *Cold Regions Science & Technology*, *44*(2), pp. 111–120. 2006. https://doi.org/10.1016/j.coldregions.2005.09.003

[20] Ling, X. Z., Zhu, Z. Y., Zhang, F., Chen, Sj., Wang, Ln., Gao, X., Lu, Qr. "Dynamic elastic modulus for frozen soil from the embankment on Beiluhe Basin along the Qinghai–Tibet Railway". *Cold Regions Science & Technology*, *57*(1), pp. 7–12. 2009. https://doi.org/10.1016/j.coldregions.2009.01.004

[21] Zhang, F. "Dynamic response and permanent of subgrade influenced by heavy truck load in deep seasonally frozen region". Ph.D. Thesis. Harbin: Harbin Institute of Technology.pp. 1. 31–58. 2012. (In Chinese with English abstract)

[22] Perreault P, Shur Y. "Seasonal Thermal Insulation to Mitigate Climate Change Impacts on Foundations in Permafrost Regions". *Cold Regions Science & Technology*, *132*, pp. 7–18. 2016. https://doi.org/10.1016/j.coldregions.2016.09.008

[23] Ministry of Housing and Urban-Rural Development of the People's Republic of China. "Standard of soil test method (GB/T50123-1999)". Beijing: China Planning Press.pp. 16–22, 143–145. 1999. (In Chinese with English version)

[24] Wang, D. Y., Zhu, Y. L., Wei, M., Niu, Y. H. "Application of ultrasonic technology for physical–mechanical properties of frozen soils". *Cold Regions Science & Technology*, *44*(1), pp. 12–19. 2006. https://doi.org/10.1016/j.coldregions.2005.06.003

[25] Hardin, B. O., Drnevich, V. P. "Shear modulus and damping in soils: Measurement and parameter effects". *Journal of the Soil Mechanics and Foundations Division, ASCE*, *98*(6), pp. 603–624. 1972.